Digest Journal of Nanomaterials and Biostructures Vol. 10, No. 3, July - September 2015, p. 769 - 777

HYDROTHERMAL SYNTHESIS OF MAGNETIC $CoFe_2O_4$-GRAPHENE NANOCOMPOSITE WITH ENHANCED PHOTOCATALYTIC PERFORMANCE

C. SUWANCHAWALIT[a*],V. SOMJIT[a]
[a]*Department of Chemistry, Faculty of Science, Silpakorn University, Sanam Chandra Palace Campus, Nakornpathom, Thailand 73000*

A magnetic $CoFe_2O_4$-graphene nanocomposite was prepared via a facile one-pot hydrothermal method and characterized by X-ray powder diffraction (XRD), diffuse reflectance UV-vis spectroscopy (DRS), scanning electron microscopy (SEM), Fourier transform infrared spectroscopy (FTIR), and vibrating sample magnetometry (VSM) techniques. The $CoFe_2O_4$ nanoparticles were found to have a size of ca. 15 nm and were spread out on the graphene sheet. Magnetic studies revealed that the $CoFe_2O_4$-graphene nanocomposites can be easily separated from the solution by an external magnetic field. The photocatalytic degradation of methylene blue dye (MB) was evaluated under visible irradiation. The photocatalytic activity was found to be affected by the structural and optical properties as well as the surface area of the samples. Compared with pure $CoFe_2O_4$, the $CoFe_2O_4$-graphene nanocompositeexhibited improved photodegradation performance. The synthesized $CoFe_2O_4$-graphene nanocomposite can be potentially used as a visible-light responsive magnetically separablephotocatalyst and hence as a powerful separation tool to deal with water pollution problems.

(Received May 21, 2015; Accepted July 10, 2015)

Keywords:$CoFe_2O_4$-graphene nanocomposite,Magnetic nanocomposite, Visible photocatalyst,Degradation of dye

1. Introduction

Recently, semiconductor-based photocatalysis has shown great potential inwastewater treatment due to its high efficiency in the degradation of various water pollutants [1,2]. Nano-semiconductor photocatalysts offer an extremely convenient route for eliminating the various organic pollutants which can be easily degraded under UV or solar light irradiation in the presence of photocatalysts [3, 4].It is well known that it is difficult to separate and recover the nano-sized photocatalysts from the solutions by a simple approach. Therefore, the nanoparticles in water would lead to a second contamination. Magnetic separation is an effective method to recover the magnetic particles by an applied magnetic field. Recently, magnetic photocatalysts composed of magnetic particles and photocatalysts have attracted great interest[5,6].

Spinel ferrites (MFe_2O_4, M = metal cation) are chemically and thermally stable magnetic materials with small band gaps (~2 eV),making them active under visible light irradiation [7,8].Cobalt ferrite ($CoFe_2O_4$) is a class of semiconductors with narrow bandgaps, exhibits characteristics of visible-light response, possesses good photochemical stability, as well as favorable magnetism[8,9]. The presence of $CoFe_2O_4$ magnetic nanoparticles fairly enhances the efficiency of the degradation of organic contaminants and can be easily separated from the solution by applying an external magnetic field.

*Corresponding author: suwanchawalit_c@su.ac.th

The main drawback of pure semiconductor photocatalysts isthat the photo generated electron–hole pairs have faster recombinationrates,which will reduce the photocatalytic efficiency of the semiconductor photocatalysts [10,11].One of the effective ways to solve this problem is to prepare semiconductor nanocomposites, which will facilitate the charge migration [12].Carbonaceous materials have been widely utilized for modifyingsemiconductor photocatalysts for effectively transporting electrons [13, 14].Graphene, an atomic sheet of sp^2 bonded carbon atoms, with a large specific surface area, remarkable electrical conductivity, excellent adsorptivity, and high chemical and thermal stability, has attracted a great deal of interest in the field of photocatalysis [15]. Therefore graphene can be used as an ideal high performance candidate for the charge migration during the photocatalysis process.

In this research, magnetic $CoFe_2O_4$-graphene nanocomposites were synthesized by the hydrothermal method using graphite powders, $FeCl_3$•$6H_2O$ and $CoCl_2$•$6H_2O$ as precursors. The microstructure, optical properties, and magnetic properties of the synthesized $CoFe_2O_4$-graphene nanocomposites were investigated. The photocatalytic activity of the as-prepared $CoFe_2O_4$-graphene nanocomposites was evaluated using methylene blue as a model pollutant.

2. Experimental Procedure

2.1Preparation of $CoFe_2O_4$

Magnetic $CoFe_2O_4$ nanoparticles were prepared via a one-pot hydrothermal method.Briefly, a 4 mmol of $FeCl_3$•$6H_2O$ solution was mixed with 0.078 M glycerol under stirring. After mixing well, an aqueous solution of 2 mmol of $CoCl_2$•$6H_2O$ was slowly added to the above mixture to give a uniform solution. The pH was then adjusted to 10 by dropwise addition of 6 M NaOH aqueous solution. Then the mixture was transferred to a Teflon-lined autoclave and kept at 200 ^{o}C in a furnace for 6 h. Finally, the precipitate was collected, centrifuged and washed several times with distilled water, then dried at 100 ^{o}C for 6 h.

2.2Preparation of $CoFe_2O_4$-graphene nanocomposites

The graphene oxide (GO) was synthesized using the modified Hummers method through oxidation of graphite powder [16,17].The hydrothermal method was employed to synthesize the $CoFe_2O_4$-graphene nanocomposites. Briefly, 1000 mg of GO was dispersed into 50 mL of distilled water with sonication for 1 h before 200 mg $CoFe_2O_4$ suspension was added and the mixture stirred for 30 min at room temperature to produce a $CoFe_2O_4$-GO dispersion. The resulting mixture was transferred to a 100 mL Teflon-lined stainless steel autoclave and heated to 200 ˚C for 5 h under autogenous pressure. The reaction mixture was allowed to cool to room temperature and the precipitate was filtered, washed five times with distilled water and dried in a vacuum oven at 60 ˚C for 12 h.

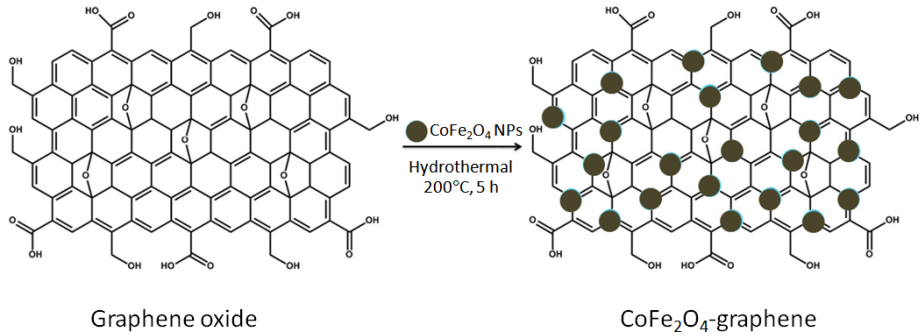

Fig. 1The procedure of $CoFe_2O_4$-graphene nanocomposite preparation by the hydrothermal method

2.3 Characterizations

The crystal structure and crystallite size were identified by X-ray diffraction (XRD) patterns recorded on a Rigaku MiniFlex II X-Ray diffractometer with Cu Kα radiation (1.5406 Å) from 20° to 70° (2θ). The particle morphologies and microstructure were investigated using a scanning electron microscopy (SEM, JEOLmodel JSM-7800F and TEM, JEOL,JEM-2010). Fourier-transformed infrared (FT-IR) spectra were recorded on a Perkin Elmer Spectrum Bx spectrophotometer in the range 400-4000 cm^{-1} using the KBr pellet technique. Optical absorption property and band gap energy were determined using a Shimadzu UV-2401 spectrophotometer. The magnetic hysteresis loops of samples were measured by a vibrating sample magnetometer (VSM, LakeShore Model 7404) at room temperature (300 K).

2.4 Photocatalytic experiment

The photocatalytic performances of the prepared $CoFe_2O_4$-graphene nanocomposites were evaluated by the photocatalytic degradation of methylene blue under visible light using fluorescence light 18W as a visible light source [18].The photocatalytic experiments were performed at room temperature. A 0.05 g of sample was added to 50 mL methylene blue solution (MB, $1.0x10^{-5}$M). Before the photocatalyticreaction,the suspension was stirred in the dark for 1 h to allow adsorption equilibrium of the dye onto the surface of the nanocomposites. At given irradiation time intervals, samples were collected and centrifuged to separate the nanocomposites. The residual concentration of methylene blue was monitored by the change in absorbance of the dye at 664 nm using a UV-Vis spectrophotometer (Analytik Jena GmbH).

The photocatalytic activity of the catalysts was measured interms of the degradation efficiency (%) of MB bythe following equation:

$$\text{The degradation efficiency (\%) of MB} = \frac{A_0 - A_i}{A_0} \times 100$$

where A_0 is the initial concentration of MB and $A_i$is the concentration of MB after visible lightirradiation.

3. Results and discussion

The $CoFe_2O_4$-graphene nanocomposites were synthesized by a facile one-pot hydrothermal route at 200°C for 5 h. The XRD diffraction patterns of the as-prepared $CoFe_2O_4$-graphene nanocomposites, pure $CoFe_2O_4$, graphene and graphene oxide (GO) are shown in Fig. 2. It can be seen that almost all the diffraction peaks of $CoFe_2O_4$-graphene may be assigned to the spinel-type $CoFe_2O_4$ (JCPDS 22-1086) [19].During the hydrothermal reaction, crystal growth of $CoFe_2O_4$ between the interlayer of GO destroyed the regular layer stacking, leading to the exfoliation of GO and the disappearance of the (0 0 1) diffraction peak.

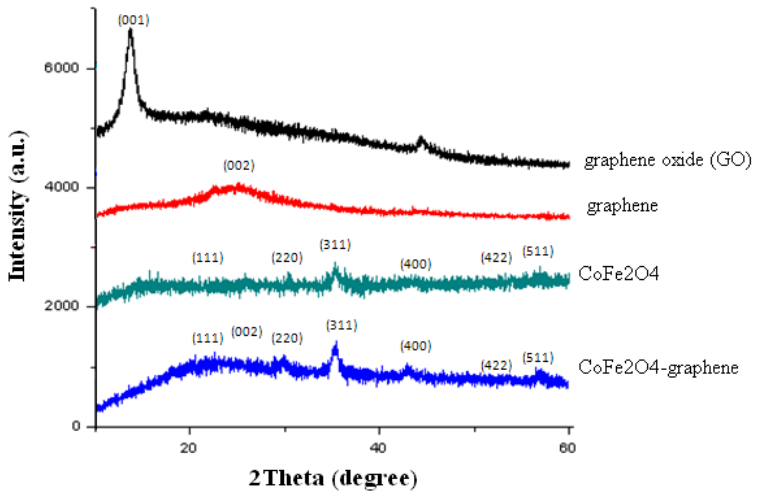

Fig. 2XRD patterns ofgraphene oxide, graphene, $CoFe_2O_4$ and $CoFe_2O_4$-graphene nanocomposite.

In order to investigate the surface chemical compositions of the obtained samples, Fourier-transform infrared spectroscopy (FT-IR) was employed, and the corresponding results are shown in Fig. 2. The FT-IR bands of $CoFe_2O_4$, observed in the range 600-500 cm^{-1}, correspond to the intrinsic stretching vibrations of the metal at the tetrahedral site Co-O stretching vibration band in $CoFe_2O_4$ and octahedral group Fe-O. The bands at 3500-3200 cm^{-1} and 1620 cm^{-1} are attributed to the stretching and bending modes of free and absorbed water on the surface of the synthesized $CoFe_2O_4$ samples [20, 21]. For the graphene spectrum, the peaks at 3400 cm^{-1}, 1723 cm^{-1}, 1630 cm^{-1}, 1370 cm^{-1}, and 1060 cm^{-1} are attributed to the OH stretching vibrations of adsorbed water, C=O stretching vibrations of carboxyl or carbonyl groups, OH deformation vibrations of COOH groups, OH deformation vibrations of tertiary C-OH, and C-O stretching vibrations of epoxy groups, respectively [22, 23].The spectrum of $CoFe_2O_4$-graphene nanocomposites exhibits the characteristic peaks due to $CoFe_2O_4$ and graphene at 536 cm^{-1}, 3400 cm^{-1}, and the oxygen-containing functional groups on the graphene sheet around 1370 cm^{-1}, and 1060 cm^{-1}, respectively.

Scanning electron microscopy (SEM) images was taken to directly analyze the morphology of the samples, as showed in Fig. 4.It can be seen thatlarge amounts of the $CoFe_2O_4$ nanoparticleswere well decorated on the graphene nanosheets in Fig. 4. To further obtain the microscopic structure information, energy-dispersive X-ray spectroscopy (EDS) and transmission electron microscopy (TEM) of $CoFe_2O_4$-graphene nanocomposites were carried out, as showed in Fig. 5 and Fig. 6.The morphology of the $CoFe_2O_4$-graphene nanocomposites was characterized by SEM and TEM observations. Figs. 4 and 5 show the representative SEM images and the corresponding EDS spectra of the as-prepared $CoFe_2O_4$-graphene nanocomposites. The EDS resultsshowed that C, Co, Fe and O elements were clearly present in the $CoFe_2O_4$-graphene nanocomposites.

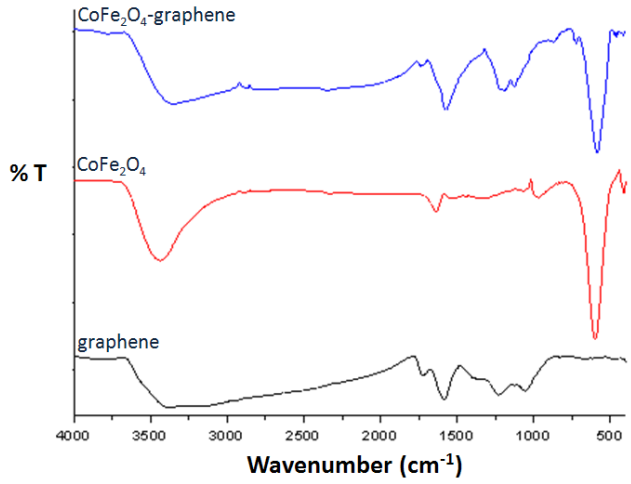

Fig. 3FT-IR spectra of prepared graphene, $CoFe_2O_4$ and $CoFe_2O_4$-graphene nanocomposites.

The TEM images of the $CoFe_2O_4$-graphene nanocomposites are shown in Fig. 6. It can be clearly seen that the flake-like graphene nanosheets are decorated with $CoFe_2O_4$ nanoparticles with some formation of aggregations. The size of the $CoFe_2O_4$ nanoparticles is uniform with an average diameter ca. 15 nm.

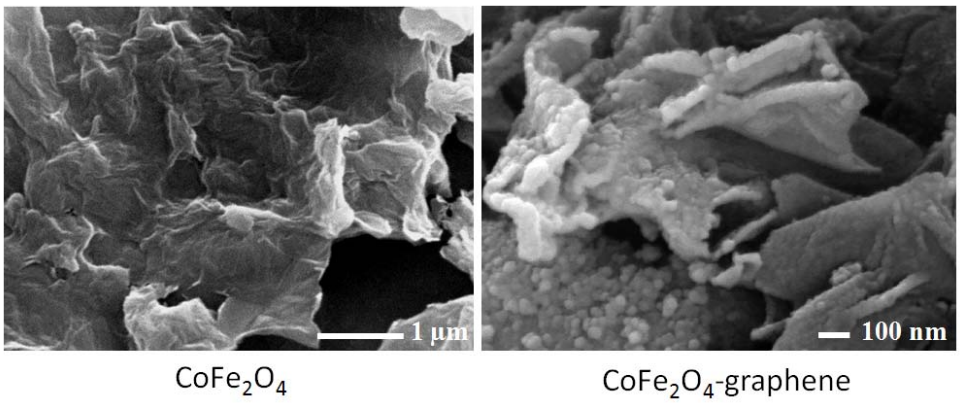

Fig. 4SEM images ofgraphene and $CoFe_2O_4$-graphene nanocomposites.

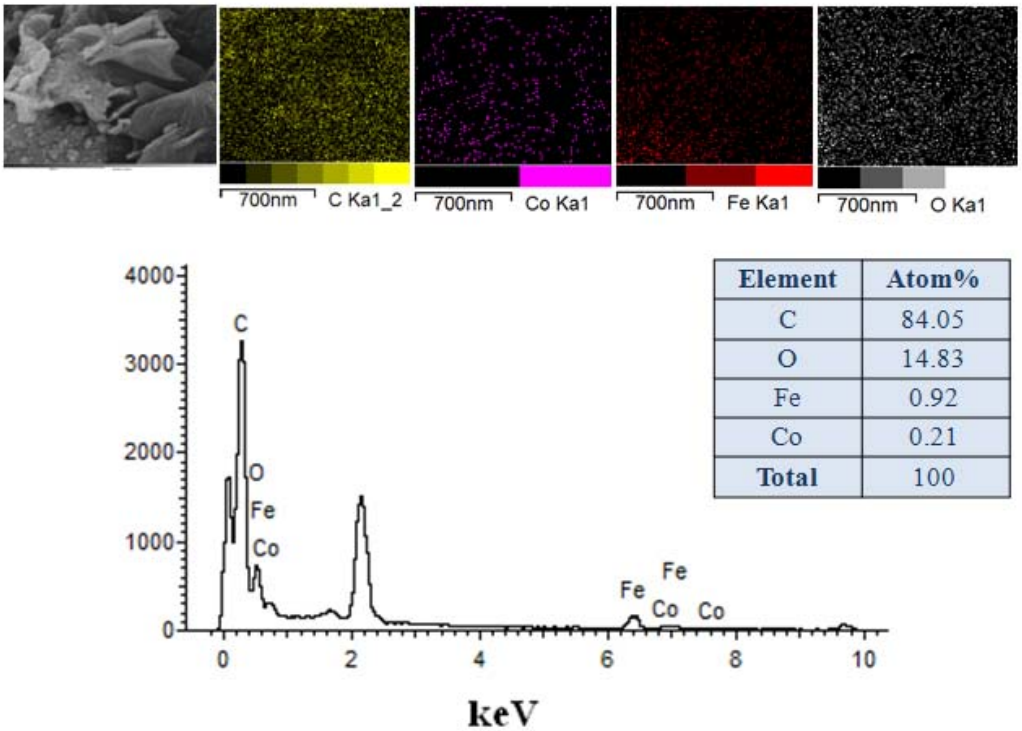

Element	Atom%
C	84.05
O	14.83
Fe	0.92
Co	0.21
Total	100

Fig. 5EDS elemental analysis and mapping analysis of $CoFe_2O_4$-graphene nanocomposites.

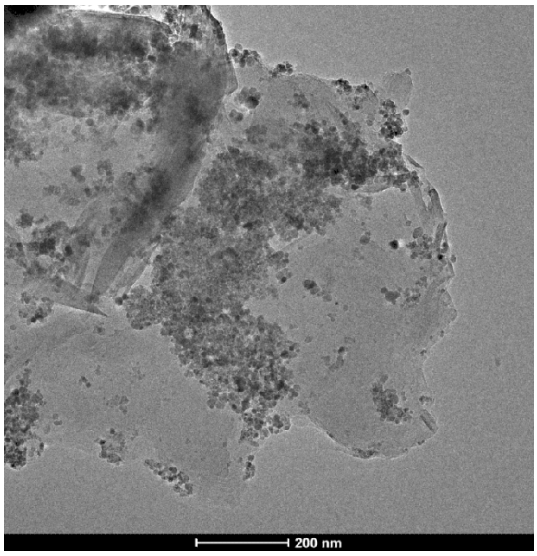

Fig. 6TEM images ofthe $CoFe_2O_4$-graphene nanocomposites.

The optical absorption property relevant to the electronic structure feature is recognized as a key factor in determining the photocatalytic activity [24].The optical properties of the prepared $CoFe_2O_4$ samples were investigated by the diffused reflectance UV-vis spectra (DRS) of the $CoFe_2O_4$, as shown in Fig. 7 (inset). According to the spectra, all synthesized $CoFe_2O_4$ samples exhibited photoabsorption from UV light to visible light region, which implies the possibility of

high photocatalytic efficiency of these materials under visible light**.** The band gap of the synthesized $CoFe_2O_4$ calculated from the plot of the transformed Kubelka-Munck function vs. the energy of light [25], is shown in Fig. 7.The band gap energies of the prepared $CoFe_2O_4$ and $CoFe_2O_4$-graphene nanocomposites are 2.28 and 2.05 eV, respectively.

The magnetization measurement for the as-prepared $CoFe_2O_4$ and $CoFe_2O_4$-graphene nanocomposites was carried out using a vibrating sample magnetometer (VSM) at room temperature. The magnetic hysteresis loops of the as-prepared $CoFe_2O_4$ and $CoFe_2O_4$-graphene nanocomposites is showed in Fig. 8, which demonstrates that the resulting samples exhibited a characteristic of ferromagnetic materials with the saturation magnetization of 22.0 and 3.8 emu g^{-1} of $CoFe_2O_4$ and $CoFe_2O_4$-graphene nanocomposites, respectively.

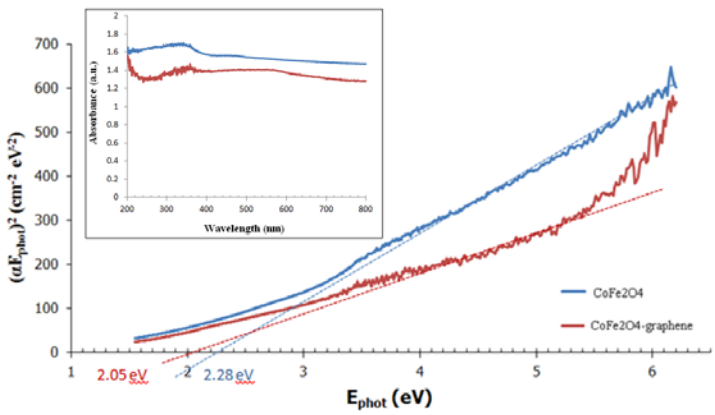

Fig. 7DRS plots of $(\alpha h\nu)^2$ vs. photon energy ($h\nu$) of the prepared $CoFe_2O_4$ and $CoFe_2O_4$-graphene nanocomposite. The top inset shows the absorption spectra of the $CoFe_2O_4$-graphene nanocomposites.

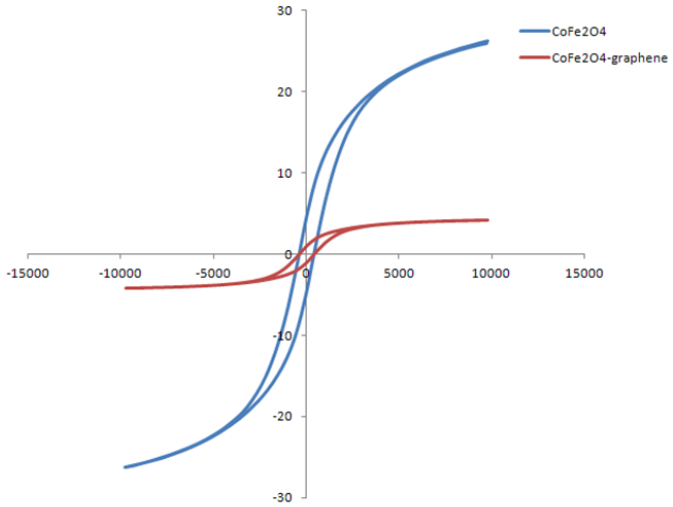

Fig. 8Hysteresis loops of the $CoFe_2O_4$ and $CoFe_2O_4$-graphene nanocomposites.

The photocatalytic degradation of methylene blue as a function of time using the synthesized $CoFe_2O_4$ and $CoFe_2O_4$-graphene nanocomposites was investigated under visible light irradiation, as shown in Fig. 9. It can be seen that the $CoFe_2O_4$-graphene nanocomposites gave the

best performance in the photocatalytic degradation of methylene blue. The $CoFe_2O_4$-graphene nanocomposites gave the highest photocatalytic efficiency due to the good optical absorptions in the UV-Vis region with a lower band gap energy and a larger surface area giving rise to a higher photocatalytic performance. In addition, the graphene in the composite can act as an electron transfer channel to reduce the recombination of the photo-generated electron holes, leading to improved photo-conversion efficiency [26, 27].

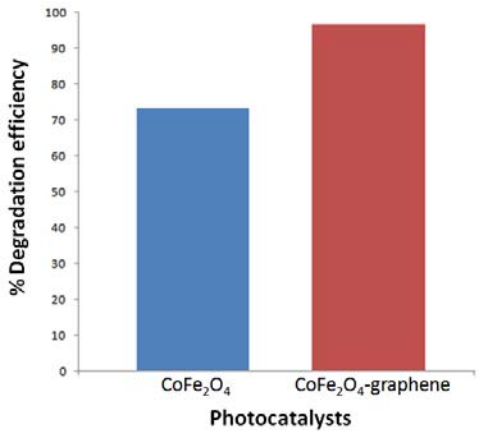

Fig. 9Comparison of the photodegradation efficiencies of methylene blue for $CoFe_2O_4$and $CoFe_2O_4$-graphene nanocomposite under visible light irradiation for 5 h.

4. Conclusion

In summary, a magnetically separable $CoFe_2O_4$-graphene photocatalyst was successfully prepared via a facile hydrothermal method. SEM, EDS and TEM results indicated that graphene sheets were fully exfoliated and decorated with $CoFe_2O_4$ nanoparticles. The photocatalytic activity measurements demonstrated that the combination of $CoFe_2O_4$ nanoparticles with the graphene sheets resulted in a dramatic conversion of the inert $CoFe_2O_4$ into a highly active catalyst for the degradation of methylene blue under visible-light irradiation. The combination of the adsorption property of the graphene sheet and the magnetic and photocatalytic property of $CoFe_2O_4$ nanoparticles makes the nanocomposites promising candidates for the solution of a variety of environmental problems.

Acknowledgments

The author would like to thank the Faculty of Science, Silpakorn University, Thailand for financial support (Grant No. SRF-JRG-2557-07).

References

[1] A. Fujishima, K. Honda, Nature.**238**, 37 (1972).
[2] M.R. Hoffmann,S.T.Martin,W.Choi,D.W.Bahnemann.,Chem.Rev. **95**, 69 (1995).
[3] P.V. Kamat, Chem. Rev. **93**, 267 (1993).
[4]Y.H. Zheng, C.Q. Chen, Y.Y. Zhan, X.Y. Lin, Q. Zheng, K.M. Wei, J.F. Zhu, J. Phys. Chem. C. **112**, 10773 (2008).
[5]D. Chen, Y. Li, J. Zhang, J.Z. Zhou, Y. Guo, H. Liu, Chem. Eng. J. **185– 186**, 120 (2012).
[6]R. Satheesh, K. Vignesh, A. Suganthi, M. Rajarajan, J. Environ. Chem. Eng.**2**, 1956 (2014).

[7] L. Cui, P. Guo, G. Zhang, Q. Li, R. Wang, M. Zhou, L. Ran, X.S. Zhao, Colloids and Interfaces A: Physicochem. Eng. Aspects. **423**, 170 (2013).
[8] Z. Zi, Y. Sun, Z. Yang, J. Dai, W. Song, J. Magn.Magn. Mater**. 321**, 1251 (2009).
[9] X.Cao, L. Gu, Nanotechnology, **16**, 180 (2005).
[10] L. Sun, J. Li, C.L. Wang, S.F. Li, Y.K. Lai, H.B. Chen, C.J. Lin, J. Hazardous Mater. **171**, 1045 (2009).
[11] H.J. Huang, D.Z. Li, Q. Lin, W.J. Zhang, Y. Shao, Y.B. Chen, M. Sun, X.Z. Fu, Environ. Sci. Technol. **43**, 4164 (2009).
[12]L. Huang, F. Peng, H.J. Wang, H. Yu, Z.Li, Catal. Commun. **10**, 1839 (2009).
[13] F. Wang, K. Zhang, J. Mole. Catal. A: Chem. **345**, 101 (2011).
[14] M. Shi, J. Shen, H. Ma, Z. Li, X. Lu, N. Li, M. Ye,Colloid Surface A. **405**, 30 (2012).
[15] H. Zhang, X.J. Lv, Y.M. Li, Y. Wang, J.H. Li, ACS Nano. **4**, 380 (2010).
[16] T. Hartono, S. Wang, Q. Ma, Z. Zhu, J. Colloid Interface Sci**. 333**, 114 (2009).
[17]P. Bradder, S. K. Ling, S. Wang, S. Liu,. J. Chem. Eng. Data. **56**, 138 (2010).
[18] C. Suwanchawalit, S.Wongnawa, P. Sriprang, P. Meanha, Ceram. Int. **38**, 5201 (2012).
[19] S. Rohilla, S. Kumar, P. Aghamkar, S. Sunder, A. Agarwal, J. Magn.Magn. Mater.**323**, 897 (2011).
[20] P. Vlazan, M. Stefanescu, P. Barvinschi, M. Stoia, Mater. Res. Bull. **47**, 4119 (2012).
[21] N. Li, M. Zheng, X. Chang, G. Ji, H. Lu, L. Xue, L. Pan, J. Cao, J. Solid State Chem**. 184**, 953 (2011).
[22] P. Wang, J. Wang, X. Wang, H. Yu, J. Yu, M. Lei, Y. Wang, Appl. Catal. B: Environ. **132-133**, 452 (2013).
[23]L. Zhou, H. Deng, J. Wan, J. Shi, T. Su,Appl. Surf. Sci.**283**, 1024 (2013).
[24] P. Sathishkumar, R.V. Mangalaraja, S. Anandan, M. Ashokkumar, Chem. Eng. J. **220**, 302 (2013).
[25] H. Guo, J. Chen, W. Weng, Q. Wang, S. Li, Chem. Eng. J. **239**, 192 (2014).
[26] D.T. Wang, X. Li, J.F. Chen, X. Tao, Chem. Eng. J. **198**, 547 (2012).
[27] K. Ullah, L. Zhu, Z.D. Meng, S. Ye, Q. Sun, W.C. Oh, Chem. Eng. J. **231**, 76 (2013).